The Kondo effect of a molecular tip as a magnetic sensor

Léo Garnier, Benjamin Verlhac, Paula Abufager, Nicolás Lorente, Maider Ormaza, Laurent Limot

The Kondo effect of a molecular tip as a magnetic sensor

Léo Garnier,[†] Benjamin Verlhac,[*,†] Paula Abufager,[‡] Nicolás Lorente,[¶,§] Maider Ormaza,[*,†] and Laurent Limot[*,†]

[†]*Université de Strasbourg, CNRS, IPCMS, UMR 7504, F-67000 Strasbourg, France*

[‡]*Instituto de Física de Rosario, Consejo Nacional de Investigaciones Científicas y Técnicas (CONICET) and Universidad Nacional de Rosario, Av. Pellegrini 250 (2000) Rosario, Argentina*

[¶]*Centro de Física de Materiales (CFM), 20018 Donostia-San San Sebastián, Spain*

[§]*Donostia International Physics Center (DIPC), 20018 Donostia-San Sebastián, Spain*

E-mail: verlhac@ipcms.unistra.fr; ormaza@ipcms.unistra.fr; limot@ipcms.unistra.fr

Abstract

A single molecule offers to tailor and control the probing capability of a scanning tunneling microscope when placed on the tip. With the help of first-principles calculations, we show that on-tip spin sensitivity is possible through the Kondo ground state of a spin $S = 1/2$ cobaltocene molecule. When attached to the tip apex, we observe a reproducible Kondo resonance, which splits apart upon tuning the exchange coupling of cobaltocene to an iron atom on the surface. The spin-split Kondo resonance provides quantitative information on the exchange field and on the spin polarization of the iron atom. We also demonstrate that molecular vibrations cause the emergence of Kondo side peaks, which, unlike the Kondo resonance, are sensitive to cobaltocene adsorption.

Introduction. The decoration of metal probe-tips by a molecule intentionally picked up from a surface has proven to be a powerful method to improve the measurement capabilities of a scanning tunneling microscope (STM). The degrees of freedom of the molecule introduce tip-surface interactions across the vacuum gap that are usually absent when using a metallic apex. These interactions can endow STM with an enhanced sub-molecular resolution,[1–3] and provide new chemical insight.[4–7] Detailed information can be gathered about single molecules on a surface and the way they interact among each other, which is of interest to chemistry and biology.[8]

To probe magnetic effects with a molecular tip it is necessary to have a magnetic molecule at the tip apex. Recently, a tip decorated with a nickelocene molecule[9] [$Ni(C_5H_5)_2$] was used to monitor surface magnetism through the inelastic component of the tunneling current,[10,11] which provides an electrical access to the nickelocene spin states.[12] An exciting alternative could consist in using a magnetic molecule undergoing a Kondo effect, which is quite common for magnetic molecules adsorbed on metal surfaces.[13] This ubiquitous quantum phenomenon occurs when a magnetic impurity —molecule or atom—couples to a non-magnetic host metal.[14] The conduction electrons of the metal spin-screen the impurity to form a singlet below a temperature T_K. The screening occurs coherently causing the emergence of a narrow resonance at the Fermi energy in the molecular conductance. Interestingly, this so-called Kondo resonance changes when the Kondo impurity magnetically couples to its local environment. By closely monitoring the resonance line shape, magnetic information can be gathered through the impurity. Kondo atoms and molecules have been widely used in STM for this purpose,[15–22] but the discrete interatomic separations imposed by the substrate lattice prevent a detailed investigation. In a seminal work to circumvent this limitation,[23] a tip was decorated with a Kondo atom and its separation from another Kondo atom on the surface was continuously changed. This study, however, suffered from the poor structural and magnetic knowledge of the tip apex. To improve tip-control and simplify the procedure, a Kondo effect carried by a molecular tip would be preferable, but its experimental

realization has remained elusive.

To build a molecular Kondo tip, we resort here to cobaltocene [$Co(C_5H_5)_2$, noted Cc] —a molecule of the metallocene family, which in vacuum has a spin $S = 1/2$ due to a singly-occupied doublet (π_{xz}, π_{yz}). We show that Cc can be sublimated onto a metal surface and subsequently picked up by the STM tip to produce reproducible Kondo physics at the tip apex. With the help of first-principles calculations and dynamical correlations, we describe the Kondo ground state and demonstrate magnetic tip-sensitivity across the vacuum gap. We also show that the Kondo signature is intertwined with molecular vibrational modes that depend on how cobaltocene is contacted to its metallic environment. The Cc-tip shows great potential for probing surface magnetism besides displaying fascinating many-body vibrational features.

Adsorption on Cu(100). After shortly exposing Cu(100) to a molecular flux (see Supporting Information), single Cc molecules were found on terraces and on step edges of the surface (Figure 1a). The Cc molecules on the terraces exhibited a ring-like pattern (inset of Figure 1b) that we assign to a cyclopentadienyl group (C_5H_5, Cp hereafter) being exposed to vacuum. The ring-like pattern observed and the apparent height of 400 ± 50 pm (Figure 1b) are typical for metallocenes,[24,25] and point to a Cc adsorbed with its molecular axis parallel to the surface normal. We found that isolated Cc was preferentially adsorbed with the bottom Cp ring centered on the hollow site of Cu(100) (see Figure S1 in Supporting Information). Our density functional theory (DFT) calculations point to a bottom Cp ring positioned at a distance of 259 pm from the surface (Figure 1c) with a 0.16 e^- charge transfer from the molecule to the substrate, which corresponds to a moderate chemisorption. The projected density of states (PDOS, Figure S2) indicates that the mixing of C(sp), Co(d_{xz}) and Co(d_{yz}) orbitals results in the partially-populated π_{xz} and π_{yz} frontier molecular orbitals, giving a magnetic character to cobaltocene on Cu(100). The computed magnetic moment of Cc is carried by the Co atom and is 0.75 μ_B, which corresponds to an effective spin of $S = 1/2$. The π orbitals are nearly degenerate and spatially add up to yield the ring-like shape of Cc

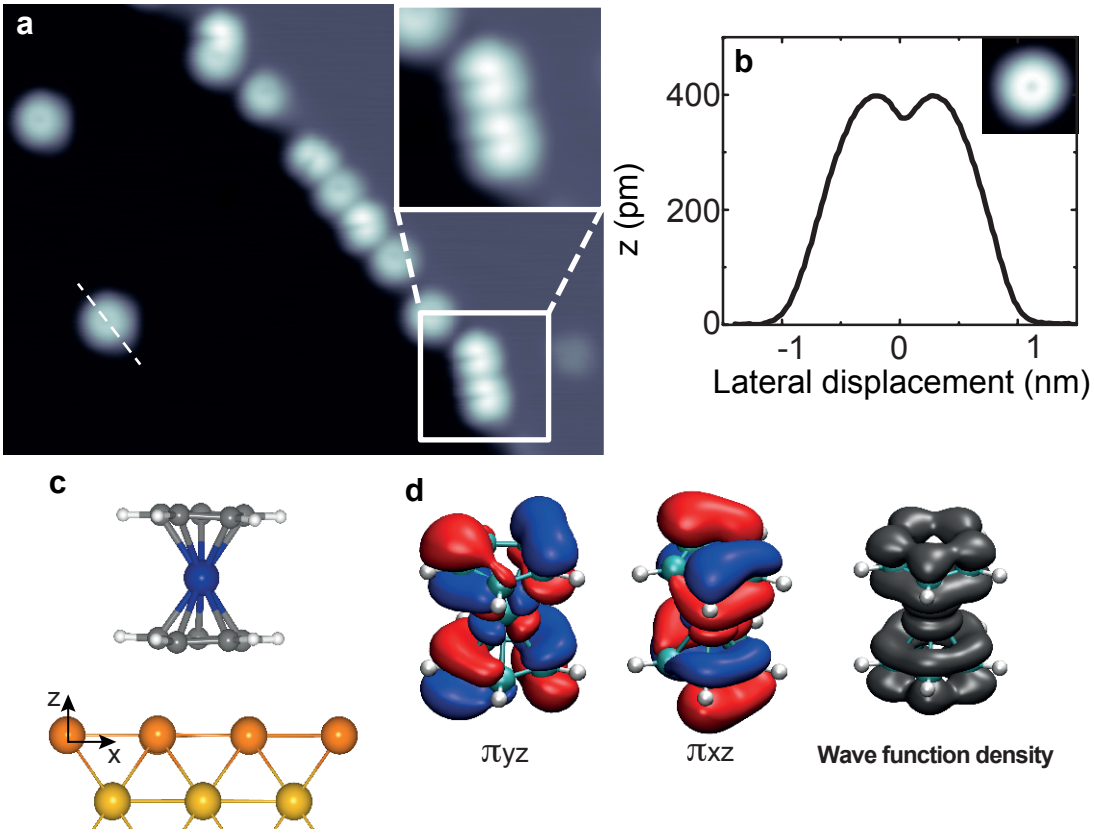

Figure 1: (a) Cobaltocene on Cu(100) (image size: 20×15 nm^2, sample bias: 20 mV, tunneling current: 30 pA). Inset: $\times 1.6$ zoom of Cc molecules at a step edge. (b) Line profile of a Cc on copper terrace. The profile was taken along the white line in panel (a). Inset: Close-up view of Cc on a terrace (2×2 nm^2, -70 mV, 20 pA). (c) Side view of the relaxed structure of Cc on Cu(100) as computed by DFT. (d) Calculated wave-function density of the π_{xz} and π_{yz} orbitals of Cc in vacuum and their linear combination.

(Figure 1d). These properties are similar to those of a nickelocene molecule that is adsorbed on a surface[25] or on a tip.[26]

Cc-tip and Kondo resonance. To prepare a Cc-tip with atomic control, we transferred a Cc from Cu(100) to the tip apex of the STM. The transfer process, which was analogous to other metallocene molecules,[9,26,27] consisted in approaching the tip towards the Cc molecule within 100 pm from point contact at a bias of -20 mV or lower (see supporting information). The presence of Cc on the tip apex produced a molecular pattern when imaging an adatom (Figure 2a), which was otherwise featureless when using a metallic tip apex (Figure S1). The molecular pattern is attributed to a Cc that is adsorbed on the tip apex with its molecular axis tilted with respect to the surface normal. Three configurations were observed: a two-lobe pattern with one lobe brighter than the other (noted **1**), a two-lobe pattern with equal intensities on the lobes (**2**), and a one-lobe pattern (**3**).

We used DFT to compute the structure of the Cc-tip. We mimicked the molecular tip by considering a Cc molecule adsorbed on a Cu adatom on Cu(100) (Figure 2b) and calculated the relaxed structure (see Supporting Information). We found an excellent agreement between the experimental and the simulated STM images (Figure 2c). The relaxed structures correspond to three stable configurations close in energy (Table S1). Configuration **1** and **3** correspond to a Cc bound to the Cu adatom trough two C atoms of the Cp ring, resulting in a tilt angle of 16° with respect to the surface normal. Configuration **2** corresponds to a Cc bound to the Cu adatom through one C atom of the Cp ring, resulting in a tilt angle of 4°. We note that similar stable configurations, where a Cu atom either interacts with a C-C bond or a with C atom, are also observed in point contact measurements of a Cu-tip with a C_{60} molecule.[28]

The computed magnetic moment of Cc on the tip shows negligible dependence on adsorption configuration (Table S1). In the case of configuration **1**, for instance, the magnetic moment is 0.89 μ_B, the projection on the Co atom giving 0.83 μ_B —the charge transfer of Cc to the metal tip is 0.12 e^-. The spin-polarized PDOS (Figure S2) changes compared to Cc

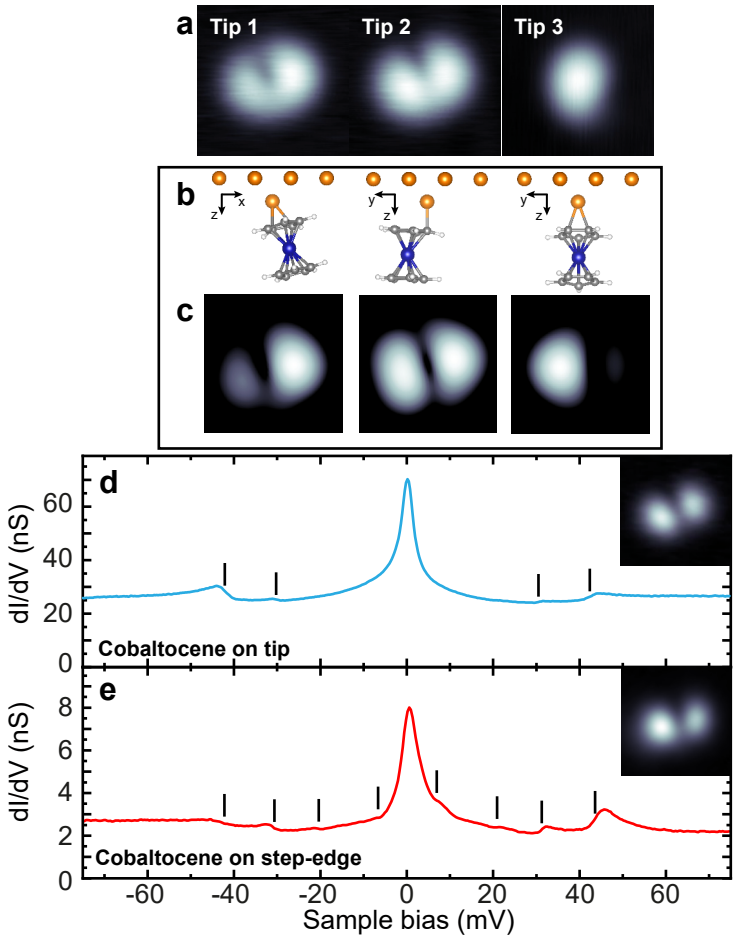

Figure 2: (a) Fe atom on Cu(100) imaged with three different Cc-tips noted **1** to **3** from left to right (1.8×1.8 nm^2, 60 mV, 30 pA). (b) DFT-computed relaxed structures for the Cc-tip, and, (c) corresponding simulated STM images (0.8×0.8 nm^2, isovalue: 0.004 nm^{-3}). (d) dI/dV spectrum taken with a Cc-tip above the bare Cu(100) surface (feedback loop opened at -70 mV, 200 pA). Inset: Constant-height dI/dV image acquired with the Cc-tip above a Fe atom (1.6×1.6 nm^2, sample bias: -2 mV). The feedback loop was opened at distance of $z = 0.4$ nm above the center of the Fe atom. (e) dI/dV spectrum of a Cc adsorbed at a step edge of Cu(100) surface acquired with a Cu-terminated tip (-75 mV and 200 pA). Inset: Constant-height dI/dV image acquired above a Cc adsorbed at a step edge (2.5×2.5 nm^2, sample bias: $+4$ mV). The feedback loop was opened at distance of $z = 0.4$ nm above one of the Cc lobes. The vertical lines in panels (d) and (e) mark the position of Kondo side peaks due to molecular vibrations.

on the copper surface. The effective spin $S = 1/2$ of the Cc-tip is now carried by an unpaired electron in the π_{yz} orbital, which corresponds to a singly occupied molecular orbital. The π_{xz} orbital lies above the Fermi energy and corresponds to the lowest unoccupied molecular orbital. The π_{yz} orbital possesses a nodal plane perpendicular to the Cp ring (Figure 1d) and produces the two-lobe pattern seen in the STM images of the Cc-tip. This behavior is common to other cobaltocene derivatives.[29]

Figure 2d presents a typical differential conductance (dI/dV) spectrum that was acquired with Cc-tip **2** positioned above a Cu(100) terrace. The spectrum exhibited a sharp peak near zero-bias and was flanked by peaks nearly symmetric with bias polarity (solid black lines in Figure 2d). The dominant zero-bias peak is assigned to a Kondo resonance resulting from the spin-flip scattering of tip conduction electrons by the $S = 1/2$ spin of Cc. The nearly symmetric shape of the peak indicates that the quantum interference with the continuum of the tip electrons is negligible.[30] The spatial distribution of the Kondo resonance in the molecule (inset of Figure 2d) follows the two-lobe pattern of the π_{yz} orbital, revealing that the Kondo effect is carried by this orbital.

The side peaks are assigned to a Kondo effect where tunneling electrons have their spin flipped when elastically scattering off the Cc spin, but with sufficient energy to activate a vibrational mode in the molecule.[31] These peaks fall at biases corresponding to the vibrational excitation energies of the cobaltocene molecule.[32–36] Their intensity is higher at negative bias compared to positive bias. Additionally, while the Kondo resonance showed little dependence on tip configuration (Figure S3), the intensity of these side peaks changed from tip to tip. For simplicity, in the following we restrain the presentation to Cc-tip **2** without loss of generality. To enrich the discussion of the Kondo line shape, we include in our analysis the Cc molecules that are adsorbed at the bottom of the edge of Cu(100) steps (inset of Figure 1a; see also Figure S1). Remarkably, these Cc have same experimental markers as the Cc-tip. They have a two-lobe pattern when imaged and their dI/dV spectrum is nearly mirror symmetric in bias to the spectrum acquired with a Cc-tip (Figure 2e).

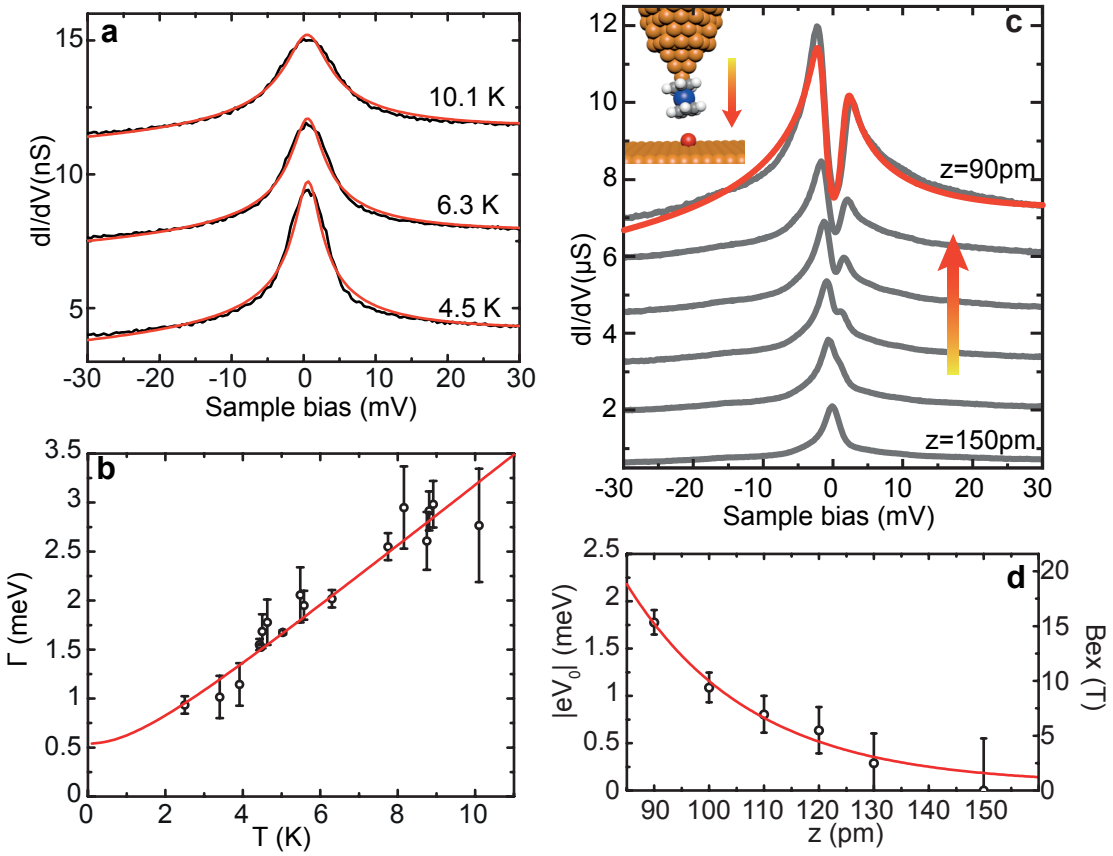

Figure 3: (a) dI/dV spectra of Cc adsorbed on a step-edge of Cu(100) for different temperatures (feedback loop opened at -70 mV, 300 pA). For clarity, the middle and top spectra are shifted vertically by 4 and 8 nS, respectively. The solid red lines are simulated line shapes using Eq. (1) with $\epsilon_K = 0.5 \pm 0.1$ meV. (b) Temperature-dependence of Γ extracted from the dI/dV spectra. The solid line correspond to the curve calculated using Eq. (2). (c) Set of dI/dV spectra acquired with the Cc-tip positioned above a Fe for various tip-atom distances; for clarity, the spectra were shifted vertically from one another by 1 μS. The distance $z = 0$ corresponds to point contact (Figure S4). The solid red lines are a line shape simulation based on a dynamical scattering model.[37,38] We used the third-order formulas to include Kondo physics and set the potential scattering U to zero. Inset: Sketch of the experimental setup. (d) Distance dependence of the excitation threshold $|eV_0|$ (y-axis: left) and of the exchange field (y-axis: right). The exponential fit described in the text is plotted as a solid red line.

Cc-tip: Kondo effect. To validate the Kondo nature of the zero-bias peak, we probed the temperature dependence of the dI/dV spectrum of the Cc-tip and that of the Cc at the step edge. A set of spectra is presented Figure 3a. The peak broadened progressively with temperature, which is a signature of a Kondo system. The dI/dV spectra were simulated using a Frota function (solid red line in Figure 3a)[39,40]

$$\sigma(eV,\Gamma) = h * \Re\left[\sqrt{i\Gamma/(i\Gamma + eV - \epsilon_{\mathrm{K}})}\right] + \sigma_0, \tag{1}$$

where $\Re$ indicates the real part, while σ_0, h and ϵ_{K} are constants. The thermal smearing introduced by the tunneling mechanism and the smearing of the lock-in detection were also accounted for in the simulation.[41] As shown in Figure 3b, the evolution of $\Gamma(T)$ with temperature is well reproduced by[42]

$$\Gamma(T) = 1.455/2\sqrt{(2k_{\mathrm{B}}T_{\mathrm{K}})^2 + (\alpha k_{\mathrm{B}}T)^2}, \tag{2}$$

where k_{B} is the Boltzmann constant. We obtain $T_{\mathrm{K}} = 4.3 \pm 1.3$ K and $\alpha = 5.0 \pm 0.3$ (solid line in Figure 3b). This asymptotic slope is close to the predicted value for a spin-1/2 Kondo system in the strong coupling regime,[42] while the relatively small value of T_{K} indicates a weak coupling of Cc to the metal tip apex. Similar findings were reported for other Kondo systems.[43,44]

To further evidence the Kondo nature the zero-bias peak, we magnetically coupled the Cc-tip to a Fe atom on Cu(100) across the vacuum gap. The magnetic coupling of a Kondo atom to another magnetic atom,[16,23] or a magnetic electrode,[19,45] is known to split the Kondo resonance into two peaks. A typical set of dI/dV spectra recorded above the Fe atom at different tip-atom distances z is presented in Figure 3c ($z = 0$ corresponds to point contact, Figure S4). The spectra were acquired with one of the lobes of the Cc-tip centered on the atom. While the $z = 150$ pm spectrum was indistinguishable from the one acquired above the bare Cu(100), for smaller distances a splitting of the peak was apparent. The splitting

became increasingly stronger as z was decreased, the median energy position of the two peaks remaining unchanged within experimental resolution. However, the intensity of the two peaks was asymmetric for opposite voltage polarities.

To rationalize these observations, we follow our previous work on the nickelocene-terminated tip,[11] and use a simplified spin Hamiltonian to describe the magnetically coupled Cc-Fe system (see supporting information and Figure S5):

$$\hat{H} = -g\mu_{\mathrm{B}} B_{\mathrm{ex}} \hat{S}_z, \tag{3}$$

where the z-axis corresponds to the out-of-surface direction —for simplicity, we neglect the small tilt angle of Cc. Even though Kondo correlations are not explicitly accounted for in Eq. (3), similar spin Hamiltonians have been shown to quantitatively describe the energies of spin-split Kondo peaks.[16,20,37,43] This effective Zeeman Hamiltonian consists of the gyromagnetic factor ($g = 2$), the Bohr magneton ($\mu_{\mathrm{B}} = 57.9\ \mu\mathrm{eV/T}$), and the exchange field (B_{ex}) produced by the Fe atom and acting on Cc along the z-axis. Within mean-field theory, $B_{\mathrm{ex}} = |J|\langle S_{\mathrm{z,Fe}}\rangle / g\mu_{\mathrm{B}}$, where $\langle S_{\mathrm{z,Fe}}\rangle \approx 3/2$ is the effective spin of Fe on copper[11,46] and J is the magnetic coupling between Cc and Fe —we take the coupling to be Ising-like. The spin-split zero-bias peak is then ascribed to a pair of conductance steps placed symmetrically about zero bias. The steps in Figure 3c are associated to inelastic tunneling events in which tunneling electrons excite Cc from its magnetic ground state $|m = +1/2\rangle$, with m as the magnetic quantum number, to the excited state $|m = -1/2\rangle$. They are located at a bias $|eV_0| = g\mu_{\mathrm{B}} B_{\mathrm{ex}}$ corresponding to the energy separating the two Zeeman levels.

A line shape simulation based on Eq. (3) and on a dynamical scattering model[37,38] is presented as a solid red line in Figure 3c. The simulated line closely reproduces the experimental spectra. Figure 3d presents quantitative estimates for B_{ex} as extracted from the simulations carried out at various distances z. The exchange field is an exponential function of z of the form $\exp(-z/\lambda)$ (Figure 3d) with a decay length of $\lambda = (23 \pm 1)$ pm, which

is characteristic of an exchange interaction across a vacuum gap.[10,11,47–49] The coupling is $|J| \approx 1.3$ meV at the shortest probed Fe-Cc distance, similar to other exchange coupled systems.[45,50] Our simulations also capture the line shape asymmetry observed experimentally. This asymmetry $\eta = (h_+ - h_-)/(h_+ + h_-)$, which stems from a selection rule for spin excitations,[38,51] reflects changes in the inelastic step height at positive and negative voltage (h_+ and h_-). From our simulations, we found a constant value of $\eta = 20 \pm 5\%$ for the shortest tip-sample distances (solid lines in Figure 3c). Although this value must be handled with care as the potential scattering was set to zero in our simulations,[20] η provides a measure for the adsorbate-related spin polarization owing to the Kondo nature of the Cc-tip.[20,52] With the help of an external magnetic field, the information gathered at the atomic-scale with a Cc-tip, either through the exchange interaction or the spin polarization, should prove sufficient for obtaining a magnetic contrast in STM images.

Cc-tip: Kondo side peaks. The coupling of the singly-occupied π_{yz} orbital to molecular vibrations leads to Kondo side peaks. These peaks are highlighted in the d^2I/dV^2 spectrum in Figure 4a acquired with a Cc-tip in configuration **2** (the spatial dependence of the most salient mode is shown in Figure S6). The peak positions, which, as expected,[53] are symmetric with bias polarity, are marked by a vertical line in the spectra. Figure 4b summarizes all the peak positions observed experimentally in an energy range up to 50 meV, including the peak positions observed in the spectra for Cc at the step edge (shown in Figures S7,S8). The peak positions, hence the energies of the vibrational modes, show negligible dependence on Cc adsorption or intramolecular position. Their intensity, instead, may change substantially (Figures S7), which hints to modes having different electron-vibration couplings. This is apparent when simulating the Kondo spectral function (Figure 4c, see Supporting Information), where we fixed the position of the side peaks to the DFT-computed vibrational energies of configuration **2** (Figure 4b; all computed configurations are presented in Figure S8). A satisfying agreement with experiment is found, but clearly some modes are favored in the experimental line shape due to a stronger electron-vibration coupling. Further work will be

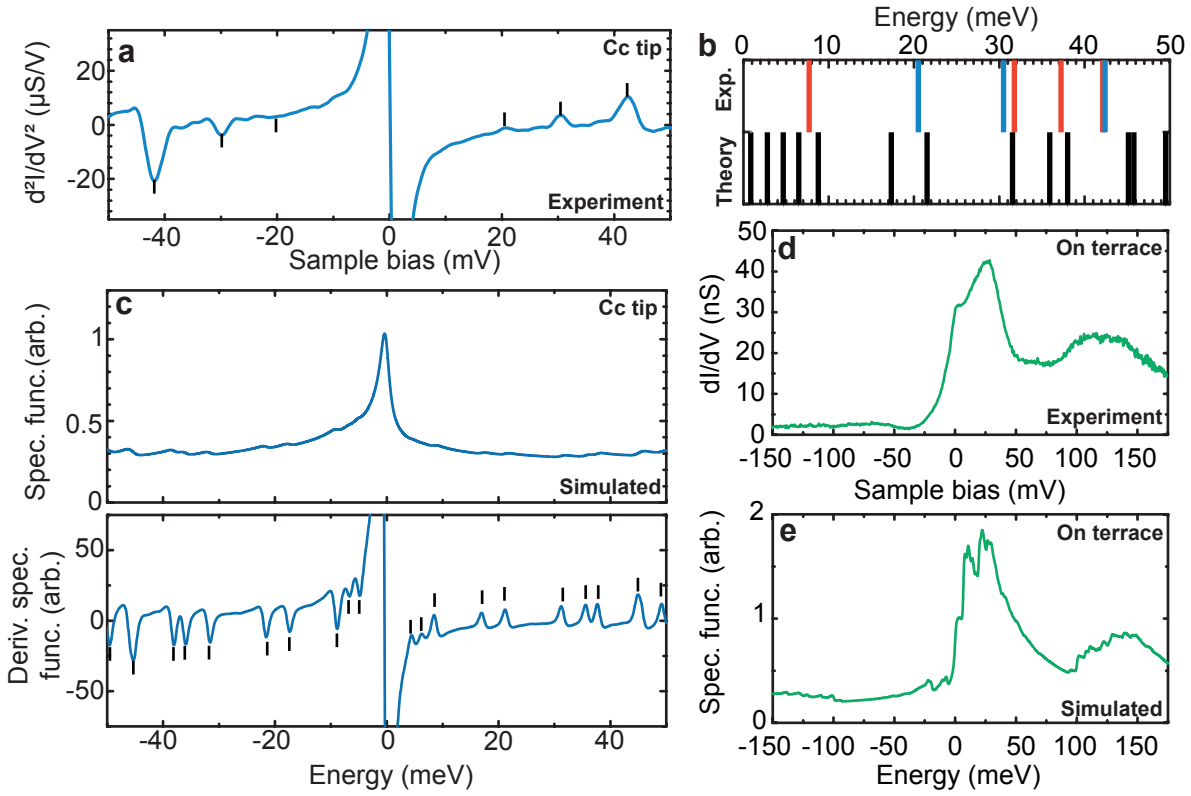

Figure 4: (a) d^2I/dV^2 spectrum of a Cc-tip in configuration **2** (feedback loop opened at -70 mV and 2 nA). (b) Experimental (x-axis: top) and DFT-computed (x-axis: bottom) vibrational energies. The experimental energies comprise those of the Cc-tip (blue lines) and of Cc at the step edge (red lines). (c) Computed spectral function of a Cc-tip in configuration **2** (top panel) and its derivative (bottom panel). (d) dI/dV spectrum of Cc adsorbed on a terrace of Cu(100). The feedback loop was opened at -175 mV, 200 pA. (e) Computed spectral function of Cc with a quasi-continuum of vibrational excitations (see text).

needed to understand this behavior.[54]

For a complete picture of the Kondo effect of cobaltocene, we present in Figure 4d a typical dI/dV spectrum of single-Cc on a Cu(100) terrace. Compared to previous Cc-tip spectra, the line shape has a more complex pattern. It is much broader with a dominant peak located at 25 mV and a second peak at 125 mV, with a reproducible shoulder centered at zero-bias. The Kondo spectral function can be again computed assuming that molecular vibrations are still present when cobaltocene is adsorbed on the terrace (Figure 4e). The calculation was performed with the computed vibrational frequencies, using the Kondo temperature and the electron-vibration couplings as fitting parameters. The Kondo temperature was fixed to that of the Cc-tip, implicitly assuming that the Kondo effect is still carried by a single molecular orbital. The spectrum is broad showing two characteristic peaks at 30 mV and at 120 mV. Despite the large number of parameters, the calculation conclusively shows the prevalence of vibrational signatures in the spectrum. Unlike the Cc-tip, all possible vibrational modes of Cc are excited in the range from 2 meV to 395 meV. This leads to a quasi-continuum of excitations that are packed in two regions, one at 30 meV and the other at 120 meV, corresponding to the distribution of modes in the molecule. The low-energy features in the dI/dV can then be unambiguously assigned to a Kondo effect in the presence of strong electron-vibration coupling in the Cc molecule.

Conclusion. We have shown that by decorating a STM tip with a cobaltocene molecule it is possible to routinely produce a Kondo resonance at the tip apex, which is flanked by side peaks resulting from vibrational excitations. The Kondo resonance can be used to probe a magnetic exchange interaction across the vacuum gap and to determine a sample-related spin-polarization. These results open the exciting perspective of obtaining a magnetic contrast in the STM images by monitoring the changes in the Kondo resonance. A variety of magnetic systems can be investigated in this way, ranging from simple ones, *e.g.* atoms and molecules, to magnetic surfaces, complementing other spin-polarized scanning probe techniques.[55,56] The physics of two Kondo impurities may also be thoroughly explored with

a Cc-tip, adding control to previous work by Bork *et al.*[23] and extending it to single Kondo molecules.

Acknowledgement

The authors thank the Agence Nationale de la Recherche (grants No. ANR-13-BS10-0016, ANR-11-LABX-0058 NIE and ANR-10-LABX-0026 CSC) and the MICINN (project RTI2018-097895-B-C44) for financial support.

Supporting Information Available

Information is provided concerning tip/sample preparation and DFT calculations. Additional experimental and computational data are presented that support the main conclusions of the article (Figures S1-S8). This material is available free of charge via the Internet at `http://pubs.acs.org/`.

References

(1) Temirov, R.; Soubatch, S.; Neucheva, O.; Lassise, A. C.; Tautz, F. S. A novel method achieving ultra-high geometrical resolution in scanning tunnelling microscopy. New J. Phys. **2008**, 10, 053012.

(2) Gross, L.; Mohn, F.; Moll, N.; Liljeroth, P.; Meyer, G. The Chemical Structure of a Molecule Resolved by Atomic Force Microscopy. Science **2009**, 325, 1110–1114.

(3) Weiss, C.; Wagner, C.; Kleimann, C.; Rohlfing, M.; Tautz, F. S.; Temirov, R. Imaging Pauli Repulsion in Scanning Tunneling Microscopy. Phys. Rev. Lett. **2010**, 105, 086103.

(4) Gross, L.; Mohn, F.; Moll, N.; Schuler, B.; Criado, A.; Guitián, E.; Peña, D.; Gour-

don, A.; Meyer, G. Bond-Order Discrimination by Atomic Force Microscopy. Science **2012**, 337, 1326–1329.

(5) Chiang, C.-l.; Xu, C.; Han, Z.; Ho, W. Real-space imaging of molecular structure and chemical bonding by single-molecule inelastic tunneling probe. Science **2014**, 344, 885–888.

(6) Wagner, C.; Green, M. F. B.; Leinen, P.; Deilmann, T.; Krüger, P.; Rohlfing, M.; Temirov, R.; Tautz, F. S. Scanning Quantum Dot Microscopy. Phys. Rev. Lett. **2015**, 115, 026101.

(7) Guo, J.; Lü, J.-T.; Feng, Y.; Chen, J.; Peng, J.; Lin, Z.; Meng, X.; Wang, Z.; Li, X.-Z.; Wang, E.-G.; Jiang, Y. Nuclear quantum effects of hydrogen bonds probed by tip-enhanced inelastic electron tunneling. Science **2016**, 352, 321–325.

(8) Jelínek, P. High resolution SPM imaging of organic molecules with functionalized tips. J. Phys.: Condens. Matter **2017**, 29, 343002.

(9) Ormaza, M.; Bachellier, N.; Faraggi, M. N.; Verlhac, B.; Abufager, P.; Ohresser, P.; Joly, L.; Romeo, M.; Scheurer, F.; Bocquet, M.-L.; Lorente, N.; Limot, L. Efficient Spin-Flip Excitation of a Nickelocene Molecule. Nano Lett. **2017**, 17, 1877–1882, PMID: 28199115.

(10) Czap, G.; Wagner, P. J.; Xue, F.; Gu, L.; Li, J.; Yao, J.; Wu, R.; Ho, W. Probing and imaging spin interactions with a magnetic single-molecule sensor. Science **2019**, 364, 670–673.

(11) Verlhac, B.; Bachellier, N.; Garnier, L.; Ormaza, M.; Abufager, P.; Robles, R.; Bocquet, M.-L.; Ternes, M.; Lorente, N.; Limot, L. Atomic-scale spin sensing with a single molecule at the apex of a scanning tunneling microscope. Science **2019**, 366, 623–627.

(12) Heinrich, A. J.; Gupta, J. A.; Lutz, C. P.; Eigler, D. M. Single-Atom Spin-Flip Spectroscopy. Science **2004**, 306, 466–469.

(13) Scott, G. D.; Natelson, D. Kondo Resonances in Molecular Devices. ACS Nano **2010**, 4, 3560–3579.

(14) Hewson, A. The Kondo Problem to Heavy Fermions; Cambridge University Press: Cambridge, England, 1997.

(15) Wahl, P.; Simon, P.; Diekhöner, L.; Stepanyuk, V. S.; Bruno, P.; Schneider, M. A.; Kern, K. Exchange Interaction between Single Magnetic Adatoms. Phys. Rev. Lett. **2007**, 98, 056601.

(16) Otte, A. F.; Ternes, M.; Loth, S.; Lutz, C. P.; Hirjibehedin, C. F.; Heinrich, A. J. Spin Excitations of a Kondo-Screened Atom Coupled to a Second Magnetic Atom. Phys. Rev. Lett. **2009**, 103, 107203.

(17) Tsukahara, N.; Shiraki, S.; Itou, S.; Ohta, N.; Takagi, N.; Kawai, M. Evolution of Kondo Resonance from a Single Impurity Molecule to the Two-Dimensional Lattice. Phys. Rev. Lett. **2011**, 106, 187201.

(18) Néel, N.; Berndt, R.; Kröger, J.; Wehling, T. O.; Lichtenstein, A. I.; Katsnelson, M. I. Two-Site Kondo Effect in Atomic Chains. Phys. Rev. Lett. **2011**, 107, 106804.

(19) Fu, Y.-S.; Xue, Q.-K.; Wiesendanger, R. Spin-resolved splitting of Kondo resonances in the presence of RKKY-type coupling. Phys. Rev. Lett. **2012**, 108, 087203.

(20) von Bergmann, K.; Ternes, M.; Loth, S.; Lutz, C. P.; Heinrich, A. J. Spin Polarization of the Split Kondo State. Phys. Rev. Lett. **2015**, 114, 076601.

(21) Spinelli, A.; Gerrits, M.; Toskovic, R.; Bryant, B.; Ternes, M.; Otte, A. F. Exploring the phase diagram of the two-impurity Kondo problem. Nat. Commun. **2015**, 6, 10046.

(22) Khajetoorians, A. A.; Steinbrecher, M.; Ternes, M.; Bouhassoune, M.; dos Santos Dias, M.; Lounis, S.; Wiebe, J.; Wiesendanger, R. Tailoring the chiral magnetic interaction between two individual atoms. Nat. Commun. **2016**, 7, 10620.

(23) Bork, J.; Zhang, Y.-h.; Diekhöner, L.; Borda, L.; Simon, P.; Kroha, J.; Wahl, P.; Kern, K. A tunable two-impurity Kondo system in an atomic point contact. Nat. Phys. **2011**, 7, 901.

(24) Ormaza, M.; Abufager, P.; Bachellier, N.; Robles, R.; Verot, M.; Le Bahers, T.; Bocquet, M.-L.; Lorente, N.; Limot, L. Assembly of Ferrocene Molecules on Metal Surfaces Revisited. J. Phys. Chem. Lett. **2015**, 6, 395–400.

(25) Bachellier, N.; Ormaza, M.; Faraggi, M.; Verlhac, B.; Vérot, M.; Le Bahers, T.; Bocquet, M.-L.; Limot, L. Unveiling nickelocene bonding to a noble metal surface. Phys. Rev. B **2016**, 93, 195403.

(26) Ormaza, M.; Abufager, P.; Verlhac, B.; Bachellier, N.; Bocquet, M. L.; Lorente, N.; Limot, L. Controlled spin switching in a metallocene molecular junction. Nat. Commun. **2017**, 8, 1974.

(27) Ormaza, M.; Robles, R.; Bachellier, N.; Abufager, P.; Lorente, N.; Limot, L. On-Surface Engineering of a Magnetic Organometallic Nanowire. Nano Lett. **2016**, 16, 588–593.

(28) Schull, G.; Dappe, Y. J.; González, C.; Bulou, H.; Berndt, R. Charge Injection through Single and Double Carbon Bonds. Nano Lett. **2011**, 11, 3142–3146.

(29) Knaak, T.; Gruber, M.; Lindström, C.; Bocquet, M.-L.; Heck, J.; Berndt, R. Ligand-Induced Energy Shift and Localization of Kondo Resonances in Cobalt-Based Complexes on Cu(111). Nano Lett. **2017**, 17, 7146–7151.

(30) Fano, U. Effects of Configuration Interaction on Intensities and Phase Shifts. Phys. Rev. **1961**, 124, 1866–1878.

(31) Paaske, J.; Flensberg, K. Vibrational Sidebands and the Kondo Effect in Molecular Transistors. Phys. Rev. Lett. **2005**, 94, 176801.

(32) Yu, L. H.; Keane, Z. K.; Ciszek, J. W.; Cheng, L.; Stewart, M. P.; Tour, J. M.; Natelson, D. Inelastic Electron Tunneling via Molecular Vibrations in Single-Molecule Transistors. Phys. Rev. Lett. **2004**, 93, 266802.

(33) Parks, J. J.; Champagne, A. R.; Hutchison, G. R.; Flores-Torres, S.; Abruña, H. D.; Ralph, D. C. Tuning the Kondo Effect with a Mechanically Controllable Break Junction. Phys. Rev. Lett. **2007**, 99, 026601.

(34) Fernández-Torrente, I.; Franke, K. J.; Pascual, J. I. Vibrational Kondo Effect in Pure Organic Charge-Transfer Assemblies. Phys. Rev. Lett. **2008**, 101, 217203.

(35) Choi, T.; Bedwani, S.; Rochefort, A.; Chen, C.-Y.; Epstein, A. J.; Gupta, J. A. A Single Molecule Kondo Switch: Multistability of Tetracyanoethylene on Cu(111). Nano Lett. **2010**, 10, 4175–4180.

(36) Rakhmilevitch, D.; Korytár, R.; Bagrets, A.; Evers, F.; Tal, O. Electron-Vibration Interaction in the Presence of a Switchable Kondo Resonance Realized in a Molecular Junction. Phys. Rev. Lett. **2014**, 113, 236603.

(37) Zhang, Y.-h.; Kahle, S.; Herden, T.; Stroh, C.; Mayor, M.; Schlickum, U.; Ternes, M.; Wahl, P.; Kern, K. Temperature and magnetic field dependence of a Kondo system in the weak coupling regime. Nat. Commun. **2013**, 4, 2110.

(38) Ternes, M. Spin excitations and correlations in scanning tunneling spectroscopy. New J. Phys. **2015**, 17, 063016.

(39) Frota, H. O. Shape of the Kondo resonance. Phys. Rev. B **1992**, 45, 1096–1099.

(40) Pruser, H.; Wenderoth, M.; Dargel, P. E.; Weismann, A.; Peters, R.; Pruschke, T.;

Ulbrich, R. G. Long-range Kondo signature of a single magnetic impurity. Nat. Phys. **2011**, 7, 203–206.

(41) Crampin, S.; Jensen, H.; Kröger, J.; Limot, L.; Berndt, R. Resonator design for use in scanning tunneling spectroscopy studies of surface electron lifetimes. Phys. Rev. B **2005**, 72, 035443.

(42) Nagaoka, K.; Jamneala, T.; Grobis, M.; Crommie, M. F. Temperature Dependence of a Single Kondo Impurity. Phys. Rev. Lett. **2002**, 88, 077205.

(43) Otte, A. F.; Ternes, M.; von Bergmann, K.; Loth, S.; Brune, H.; Lutz, C. P.; Hirjibehedin, C. F.; Heinrich, A. J. The role of magnetic anisotropy in the Kondo effect. Nat. Phys. **2008**, 4, 847–850.

(44) Dubout, Q.; Donati, F.; Wäckerlin, C.; Calleja, F.; Etzkorn, M.; Lehnert, A.; Claude, L.; Gambardella, P.; Brune, H. Controlling the Spin of Co Atoms on Pt(111) by Hydrogen Adsorption. Phys. Rev. Lett. **2015**, 114, 106807.

(45) Choi, D.-J.; Guissart, S.; Ormaza, M.; Bachellier, N.; Bengone, O.; Simon, P.; Limot, L. Kondo Resonance of a Co Atom Exchange Coupled to a Ferromagnetic Tip. Nano Lett. **2016**, 16, 6298–6302.

(46) Khajetoorians, A. A.; Lounis, S.; Chilian, B.; Costa, A. T.; Zhou, L.; Mills, D. L.; Wiebe, J.; Wiesendanger, R. Itinerant Nature of Atom-Magnetization Excitation by Tunneling Electrons. Phys. Rev. Lett. **2011**, 106, 037205.

(47) Schmidt, R.; Lazo, C.; Kaiser, U.; Schwarz, A.; Heinze, S.; Wiesendanger, R. Quantitative Measurement of the Magnetic Exchange Interaction across a Vacuum Gap. Phys. Rev. Lett. **2011**, 106, 257202.

(48) Yan, S.; Choi, D.-J.; Burgess, J. A. J.; Rolf-Pissarczyk, S.; Loth, S. Control of quantum magnets by atomic exchange bias. Nat. Nanotechnol. **2014**, 10, 40.

(49) Yang, K.; Paul, W.; Natterer, F. D.; Lado, J. L.; Bae, Y.; Willke, P.; Choi, T.; Ferrón, A.; Fernández-Rossier, J.; Heinrich, A. J.; Lutz, C. P. Tuning the Exchange Bias on a Single Atom from 1 mT to 10 T. Phys. Rev. Lett. **2019**, 122, 227203.

(50) Muenks, M.; Jacobson, P.; Ternes, M.; Kern, K. Correlation-driven transport asymmetries through coupled spins in a tunnel junction. Nat. Commun. **2017**, 8, 14119.

(51) Loth, S.; von Bergmann, K.; Ternes, M.; Otte, A. F.; Lutz, C. P.; Heinrich, A. J. Controlling the state of quantum spins with electric currents. Nat. Phys. **2010**, 6, 340–344.

(52) Pasupathy, A. N.; Bialczak, R. C.; Martinek, J.; Grose, J. E.; Donev, L. A. K.; McEuen, P. L.; Ralph, D. C. The Kondo Effect in the Presence of Ferromagnetism. Science **2004**, 306, 86–89.

(53) Stipe, B. C.; Rezaei, M. A.; Ho, W. Single-Molecule Vibrational Spectroscopy and Microscopy. Science **1998**, 280, 1732–1735.

(54) Reecht, G.; Krane, N.; Lotze, C.; Zhang, L.; Briseno, A. L.; Franke, K. J. Vibrational Excitation Mechanism in Tunneling Spectroscopy beyond the Franck-Condon Model. Phys. Rev. Lett. **2020**, 124, 116804.

(55) Serrate, D.; Ferriani, P.; Yoshida, Y.; Hla, S.-W.; Menzel, M.; von Bergmann, K.; Heinze, S.; Kubetzka, A.; Wiesendanger, R. Imaging and manipulating the spin direction of individual atoms. Nature Nanotechnol. **2010**, 5, 350–353.

(56) Baumann, S.; Paul, W.; Choi, T.; Lutz, C. P.; Ardavan, A.; Heinrich, A. J. Electron paramagnetic resonance of individual atoms on a surface. Science **2015**, 350, 417–420.